Inorg. Chem. **2002**, *41*, 7159–7169

Thermally Inert Metal Ammines as Light-Inducible DNA-Targeted Agents. Synthesis, Photochemistry, and Photobiology of a Prototypical Rhodium(III)–Intercalator Conjugate

Colin G. Barry,[†] Elizabeth C. Turney,[†] Cynthia S. Day,[†] Gilda Saluta,[‡] Gregory L. Kucera,[‡] and Ulrich Bierbach*,[†]

Department of Chemistry, Wake Forest University, Winston-Salem, North Carolina 27109, and Comprehensive Cancer Center of Wake Forest University, Medical Center Boulevard, Winston-Salem, North Carolina 27157

Received May 22, 2002

The recent discovery of the promising tumor cell kill by a novel platinum–acridine conjugate [Martins, E. T.; et al. *J. Med. Chem.* **2001**, *44*, 4492] has prompted us to explore the utility of analogous light-activatable rhodium(III) compounds as photocytotoxic agents. Here, the design and synthesis of $[Rh(NH_3)_5L]^{n+}$ complexes are described with L = 1,1,3,3-tetramethylthiourea (tmtu) or 1-[2-(acridin-9-ylamino)ethyl]-1,3,3-trimethylthiourea (**2**). The intercalator-based DNA-affinic carrier ligand **2** was synthesized from *N*-acridin-9-yl-*N*′-methylethane-1,2-diamine and dimethylthiocarbamoyl chloride and isolated as the hydrotriflate salt **2**(CF_3SO_3). $[Rh(NH_3)_5(tmtu)]^{3+}$ (**1**) and $[Rh(NH_3)_5(\mathbf{2})]^{4+}$ (**3**) were obtained from the reactions of the trifluoromethanesulfonato complex $[Rh(NH_3)_5(OSO_2CF_3)](CF_3SO_3)_2$ with the appropriate thiourea in noncoordinating solvents. All compounds were characterized by ^{1}H NMR and UV–vis spectroscopies and by elemental analyses. The single-crystal X-ray structures of **1**$(CF_3SO_3)_3\cdot$2MeOH, **2**(CF_3SO_3), and **3**$(CF_3SO_3)_4\cdot H_2O$ have been determined. Ligand-field photolysis of thermally inert **1** (λ_{max} = 378 nm) resulted in the aquation of 2 equiv of ammine ligand without noticeable release of sulfur-bound tmtu (^{1}H NMR spectroscopy, NH_3-sensitive electrode measurements). This was confirmed by $^{15}N\{^1H\}$ NMR spectroscopy using ^{15}N-labeled $[Rh(^{15}NH_3)_5(tmtu)]^{3+}$ (**1***), which also indicated photoisomerization of the $[RhN_5S]$ moiety. Despite greatly accelerated ligand exchange, rhodium in **1** and **3** did not show light-enhanced formation of covalent adducts in calf thymus DNA. "Dark binding" levels of **3** in native DNA were slightly higher than for nontargeted **1**, but significantly lower than those observed for analogous platinum–acridine. Agarose gel electrophoresis revealed photocleavage of supercoiled pUC19 plasmid DNA in the presence of hybrid **3** and its individual constituents **1** and **2**. Simple **1** induced single-strand breaks while **3** produced complete degradation of the DNA after 24 h of continuous irradiation. Acridine **2** alone produced double-strand breaks. The extent of DNA damage observed for **1**–**3** correlates with the photocytotoxicity of the compounds in human leukemia cells, suggesting that DNA might be the cellular target of these agents.

Introduction

Modulation of DNA structure and DNA−protein recognition by exogenous metal complexes represents an intensively studied area of bioinorganic chemistry.[1] Transition-metal compounds that bind to DNA in a covalent or noncovalent fashion or induce DNA strand scission have potential applications as tools for probing biomolecular structure and function and as cytotoxic agents in cancer chemotherapy.[2] Kinetic lability/inertness toward ligand substitution is a major determinant that controls the covalent interactions of a metal complex with biological target molecules. The utility of a

* Author to whom correspondence should be addressed. E-mail: bierbau@wfu.edu. Fax: (336) 758-4656.
† Department of Chemistry.
‡ Comprehensive Cancer Center.

(1) Lippard, S. J.; Berg, J. M. *Principles of Bioinorganic Chemistry*; University Science Books: Mill Valley, CA, 1994.

(2) (a) Gelasco, A.; Lippard, S. J. In *Topics in Biological Inorganic Chemistry*; Clarke, M. J., Sadler, P. J., Eds.; Springer: New York, 1999; Vol. I, p 1. (b) Piper, T.; Borsky, K.; Keppler, B. K. In *Topics in Biological Inorganic Chemistry*; Clarke, M. J., Sadler, P. J., Eds.; Springer: New York, 1999; Vol. I, p 171.

10.1021/ic025744n CCC: $22.00
Published on Web 11/27/2002

metal compound as an anticancer agent is confined to a relatively narrow kinetic window during which hydrolytic activation and exchange of aqua ligands by biological nucleophiles occurs. Among simple Werner-type transition-metal complexes, square-planar d^8 and low-spin octahedral group 8−10 complexes—especially those of platinum[3] and ruthenium[4]—are of potential interest for medical applications. In a series of metal complexes, ordered by increasing solvent exchange rates in water, divalent platinum and di- and trivalent ruthenium show intermediate kinetic lability most suitable for target-specific reactions in biological systems: Ir(III) ≪ Rh(III) ≈ Co(III) < Ru(III) < Pt(II) < Ru(II) ≪ Pd(II) ≈ Fe(III).[5] As a result, DNA-directed platinum- and ruthenium-containing agents are among the most successful and most widely studied clinical and experimental metallopharmaceuticals. In contrast, the inability of trivalent rhodium to undergo substitution reactions on a physiologically relevant time scale[5] may explain why only a few cytotoxic complexes of this metal ion are known.[4,6] Unlike trivalent ruthenium, rhodium(III) cannot be activated reductively, which has also been put forward to explain the disappointing activity profile of this metal.[2b]

While rhodium ammines, such as $[Rh^{III}(NH_3)_5X]^{2+/3+}$ (X = halide), are kinetically inert under thermal conditions, irradiation into the ligand-field (LF) bands speeds up ligand exchange by up to 14 orders of magnitude.[7,8] The leaving group specificity and photostereochemistry of ligand substitution in d^6 low-spin complexes are well understood and predictable.[9] Surprisingly, despite their interesting photochemical and photophysical properties and facile preparation, the DNA modifications by light-activated classical rhodium(III) ammines and the biological consequences thereof are widely unexplored. The only examples of light-inducible, trivalent rhodium capable of binding to DNA in a covalent fashion are compounds of the type *cis*-$[RhCl_2(polypyridyl)_2]^+$.[10] The prototype *cis*-$[RhCl_2(phen)_2]^+$ (BISPHEN; phen = 1,-10-phenanthroline) has been developed by Morrison et al., who introduced the concept of cisplatin mimics that can be activated photochemically ("photo-cisplatin").[11] The dark association of BISPHEN with calf thymus DNA was moderate ($K_i \leq 10^2$), and the compound photometalates nucleobase nitrogen with low quantum yields.[11] Furthermore, BISPHEN did not induce bifunctional adducts, unlike cisplatin, and did not produce the desired biological effects.[10] The reaction with guanine involves reductive quenching of an excited triplet ligand-field state by nucleobase-to-metal electron transfer and reoxidation of Rh(II) to Rh(III) upon covalent attachment of the metal to the N7 position.[12] Few other rhodium compounds were studied for their photochemistry in the presence of DNA. These include Rh(III)−tris-(polypyridyl) complexes and related metallointercalators[13] and dinuclear rhodium(II) carboxylates.[14] In both cases, oxidative DNA strand scission originating from ligand- or metal-centered electronic excited states is observed.[13,14]

Chart 1

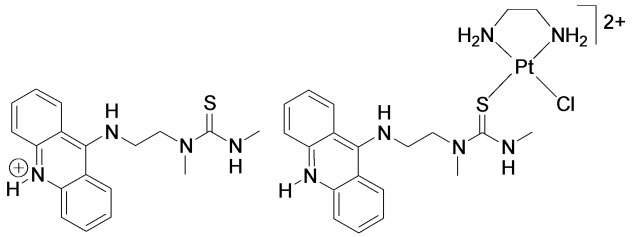

ACRAMTU **PT-ACRAMTU**

The ultimate goal of the work summarized here was to design an intercalator-tethered rhodium(III) ammine as a prototype for a DNA-targeted cytotoxic agent that can be "switched on" photochemically. Recently, we have communicated the synthesis and antitumor properties of a new sulfur-modified 9-aminoacridine, 1-[2-(acridin-9-ylamino)-ethyl]-1,3-dimethylthiourea (ACRAMTU; Chart 1), and its platinum conjugate (PT−ACRAMTU, Chart 1).[15] ACRAMTU was identified as a high-affinity DNA intercalator[16] ($K_i = 1.5 \times 10^6$ in native DNA) that, by itself, exhibits only moderate in vitro cytotoxicity in leukemia and solid tumor cell lines.[15] The attachment of the DNA metalating group $[Pt(en)Cl]^+$ (en = ethane-1,2-diamine) to sulfur in ACRAMTU resulted in dramatically increased levels of cell kill in HL-60 leukemia ($IC_{50/ACRAMTU} = 11\ \mu M$ vs $IC_{50/\ PT-ACRAMTU} = 0.13\ \mu M$).[15] These findings stimulated an interest in transferring the platinum−acridine technology to analogous conjugates of light-activatable metals. Similar to the platinum case, a dual mode involving covalent DNA damage by rhodium—in this case triggered by a photochemical rather than thermal mechanism—in addition to intercalative binding would result in biological activity several orders of magnitude higher than the "dark" cytotoxicity. Here, we present the synthesis and characterization of a prototypical rhodium−acridine agent and its interactions with DNA, which is considered a potential biological and therapeutic target of these complexes. Preliminary photocytotoxicity data for the conjugate and its individual components suggest that this type of compound, especially analogous longer-wavelength metal complexes, might have potential applications in the photochemotherapy of cancer.

(3) Wong, E.; Giandomenico, C. M. *Chem. Rev.* **1999**, *99*, 2451.
(4) Clarke, M. J.; Zhu, F.; Frasca, D. R. *Chem. Rev.* **1999**, *99*, 2511.
(5) Lincoln, S. F.; Merbach, A. E. In *Advances in Inorganic Chemistry*; Sykes, A. G., Ed.; Academic Press: New York, 1995; Vol. 42, p 1.
(6) Mestroni, G.; Zassinovich, G.; Alessio, E.; Bontempi, A. *Inorg. Chim. Acta* **1987**, *137*, 63.
(7) Kelly, T. L.; Endicott, J. F. *J. Phys. Chem.* **1972**, *76*, 1937.
(8) Magde, D.; Rojas, G. E.; Skibsted, L. H. *Inorg. Chem.* **1988**, *27*, 2900.
(9) VanQuickenborne, L. G.; Ceulemans, A. *Coord. Chem. Rev.* **1983**, *48*, 157.
(10) Billadeau, M. A.; Morrison, H. *Metal Ions Biol. Syst.* **1996**, *33*, 269.
(11) Mahnken, R. E.; Billadeau, M. A.; Nikonowicz, E. P.; Morrison, H. *J. Am. Chem. Soc.* **1992**, *114*, 9253.
(12) Harmon, H. L.; Morrison, H. *Inorg. Chem.* **1995**, *34*, 4937.
(13) (a) Erkkila, K. E.; Odom, D. T.; Barton, J. K. *Chem. Rev.* **1999**, *99*, 2777. (b) Turro, C.; Hall, D. B.; Chen, W.; Zuilhof, H.; Barton, J. K.; Turro, N. J. *J. Phys. Chem. A* **1998**, *102*, 5708.
(14) Bradley, P. M.; Patty, K. L. F.; Turro, C. *Comments Inorg. Chem.* **2001**, *22*, 393.
(15) Martins, E. T.; Baruah, H.; Kramarczyk, J.; Saluta, G.; Day, C. S.; Kucera, G. L.; Bierbach, U. *J. Med. Chem.* **2001**, *44*, 4492.
(16) Baruah, H.; Rector, C. L.; Monnier, S. M.; Bierbach, U. *Biochem. Pharmacol.* **2002**, *64*, 191.

Experimental Section

Materials. The rhodium precursors $[Rh(NH_3)_5Cl]Cl_2$ and $[Rh(NH_3)_5OSO_2CF_3](CF_3SO_3)_2$ were synthesized from $RhCl_3 \cdot xH_2O$ (Heraeus, Johnson Matthey) according to published procedures.[17,18] *N*-Acridin-9-yl-*N*′-methylethane-1,2-diamine was synthesized as described earlier.[15] For the preparation of ^{15}N-labeled rhodium pentaammine, $^{15}NH_4Cl$ (98+%, Cambridge Isotope Laboratories) was used. The rhodium standard used for inductively coupled plasma atomic emission spectrometry (ICP-AES) was from High-Purity Standards (Charleston, SC). Unless stated otherwise, organics and solvents were obtained from common vendors and used as supplied. For the preparation of biological buffers, biochemical-grade (DNase-free, where available) chemicals were used. Buffers were made from doubly distilled, 0.22 μm filtered Millipore water. Calf thymus DNA (Sigma) was purified prior to use by dialysis against the appropriate buffer using a dialysis tube with a 10000 molecular weight cutoff. The purity of calf thymus DNA was assessed spectrophotometrically from the ratio of absorbances at 260 and 280 nm.[19] Plasmid DNA (pUC19, 2686 bp, Amersham) was isolated from transformed *E. coli* DH5-α cells with the use of Qiagen Mega plasmid purification kits. The concentrations of DNA (base pairs) were determined from absorbances at 260 nm using Beer's law with $\epsilon_{260} = 12824\ M^{-1}\ cm^{-1}$ (bp).[20] DNA stock solutions were stored at 4 °C. Catalase from bovine liver was purchased from Sigma.

General Instrumentation and Procedures. ^1H NMR data were acquired on a Bruker Avance 300 spectrometer. Chemical shifts (δ, ppm) were referenced to residual solvent peaks. ^{15}N NMR spectra were measured on a Bruker Avance 500 spectrometer equipped with a tunable 5 mm broad-band probe at 50.7 MHz and referenced to 5 M $^{15}NH_4Cl$ in 2 M HCl (containing 10% D_2O), which served as external standard. Typical acquisition parameters were spectral width 7576 Hz, 32K time domain points, 500 scans, and 3 s recycle delay. A composite pulse decoupling program (waltz16) was used in $^{15}N\{^1H\}$ NMR experiments. Data were processed using a line broadening of 5 Hz. ^1H and ^{15}N NMR spectra were measured at 294 and 300 K, respectively. UV−vis spectra were taken on a Hewlett-Packard 8354 diode array spectrophotometer. The rhodium content in DNA was assessed by ICP-AES on a Perkin-Elmer Optima 3100XL ICP-emission spectrometer. Elemental analyses were performed by Quantitative Technologies, Inc., Madison, NJ.

Safety note! Triflic acid can cause severe burns. Wear suitable protective clothing and eye/face protection.

Synthesis of Pentaammine(1,1,3,3-tetramethylthiourea-*S*)-rhodium(III) Triflate, 1$(CF_3SO_3)_3$. A solution of 1.25 g (2.00 mmol) of pentaamminetriflatorhodium(III) triflate and 0.291 g (2.20 mmol) of 1,1,3,3-tetramethylthiourea (tmtu) in 10 mL of dry acetone was allowed to reflux for 24 h under argon atmosphere and protected from light. The solvent was removed under reduced pressure, and the residue was redissolved in 2 mL of dry methanol. Dry diethyl ether was added with vigorous stirring to precipitate out the crude product as an off-white solid, which was filtered off and recrystallized from methanol. Light-yellow crystals of **1**$(CF_3SO_3)_3 \cdot 2MeOH$ solvate were obtained that lose the crystal solvent upon drying of the compound at 60 °C in a vacuum. Yield: 0.982 g (64%). ^1H NMR (MeOH-d_4): δ 3.26 (12 H, s), 3.78, 3.90 (2 br s, NH_3, slow H,D exchange). UV−vis (water): λ_{max}, nm (ϵ, $cm^{-1}\ M^{-1}$): 250 (14400), 378 (580). Anal. Calcd for $C_8H_{27}F_9N_7O_9RhS_4$: C, 12.52; H, 3.55; N, 12.77; S, 16.71. Found: C, 12.54; H, 3.32; N, 12.49; S, 16.29.

The ^{15}N-labeled complex $[Rh(^{15}NH_3)_5(tmtu)](CF_3SO_3)_3$ [**1***$(CF_3SO_3)_3$] was synthesized analogously and isolated in 68% yield. $^{15}NH_3$ was introduced into the chloropentaammine precursor[17] by substituting NH_4Cl and $(NH_4)_2CO_3$ with a mixture of $^{15}NH_4Cl$ and Na_2CO_3. ^1H NMR (MeOH-d_4): δ 3.26 (12 H, s), 3.78 (12 H, d, $^{15}NH_3$, $^1J[^1H-^{15}N] = 69.7$ Hz, slow H,D exchange), 3.90 [3 H, d, $^{15}NH_3$, $^1J(^1H-^{15}N) = 70.6$ Hz, slow H,D exchange]. ^{15}N NMR (95% H_2O/5% D_2O): δ 61.96 [4 N, qd, $^1J(^{15}N-^1H) = 69.8$ Hz, $^1J(^{15}N-^{103}Rh) = 13.4$ Hz], −53.54 [1 N, qd, $^1J(^{15}N-^1H) = 70.0$ Hz, $^1J(^{15}N-^{103}Rh) = 12.5$ Hz].

Synthesis of 1-[2-(Acridin-9-ylamino)ethyl]-1,3,3-trimethylthiourea Hydrotriflate [2(CF_3SO_3)] Sample. An 8.57 g (0.034 mol) of *N*-acridin-9-yl-*N*′-methylethane-1,2-diamine was dissolved in 100 mL of dry THF. A solution of 2.11 g (0.017 mol) of dimethylthiocarbamoyl chloride in 20 mL of dry THF was added dropwise within 10 min with stirring, and the mixture was allowed to reflux for 4 h. Stirring and heating were discontinued, and the mixture was allowed to sit overnight. The precipitate (*N*-acridin-9-yl-*N*′-methylethane-1,2-diamine hydrochloride) was collected by filtration. To the filtrate was added 1.51 mL (2.55 g, 0.017 mol) of trifluoromethanesulfonic acid, and the mixture was stored for 12 h at 4 °C. A 7.18 g sample of crude product was recovered as a brown-yellow crystal mass and recrystallized from hot ethanol, yielding 6.16 g (74%) of bright-yellow needles of **2**(CF_3SO_3). ^1H NMR (MeOH-d_4): δ 3.02 (6 H, s), 3.05 (3 H, s), 4.25 (2 H, t), 4.54 (2 H, t), 7.56 (2 H, t), 7.81 (2 H, d), 7.97 (2 H, t), 8.65 (2 H, d). UV−vis (water): λ_{max}, nm (ϵ, $cm^{-1}\ M^{-1}$) 221 (24200), 257 (52800), 266 (53600), 370 (sh), 395 (6460), 414 (10200), 436 (8760). Anal. Calcd for $C_{20}H_{23}F_3N_4O_3S_2$: C, 49.17; H, 4.75; N, 11.47; S, 13.13. Found: C, 49.48; H, 4.71; N, 11.36; S, 13.14.

Synthesis of Pentaammine{9-[2-(trimethylthioureido)ethylamino]acridinium-*S*}rhodium(III) Triflate, 3$(CF_3SO_3)_4$. A 0.251 g (0.514 mmol) sample of **2**(CF_3SO_3) was dissolved in 15 mL of pentan-3-one (dried over 4 Å molecular sieves), and the mixture was heated until all of the compound was dissolved. A 0.326 g (0.514 mmol) sample of pentaamminetriflatorhodium(III) triflate in 5 mL of dry pentan-3-one was added, and the mixture was allowed to reflux for 48 h under argon atmosphere in the dark. **3**$(CF_3SO_3)_4$ precipitated in the heat. The solution was allowed to slowly cool to room temperature, and the product was collected by filtration and dried at 60 °C in a vacuum. Yield: 0.370 g (64%) of a bright-yellow microcrystalline solid. ^1H NMR (MeOH-d_4): δ 3.17 (6 H, s), 3.25 (3 H, s), 4.26 (2 H, t), 4.61 (2 H, t), 7.63 (2 H, t), 7.88 (2 H, d), 8.02 (2 H, t), 8.53 (2 H, d). UV−vis (water): λ_{max}, nm (ϵ, $cm^{-1}\ M^{-1}$) 223 (30100), 266 (75000), 332 (2890), 375 (sh), 397 (7810), 415 (10590), 437 (8230). Anal. Calcd for $C_{23}H_{38}F_{12}N_9O_{12}RhS_5$: C, 24.58; H, 3.41; N, 11.22; S, 14.27. Found: C, 24.09; H, 3.19; N, 10.80; S, 13.95.

X-ray Crystallographic Analysis of 1$(CF_3SO_3)_3 \cdot 2MeOH$, 2(CF_3SO_3), and 3$(CF_3SO_3)_4 \cdot H_2O$. Suitable single crystals of **1**$(CF_3SO_3)_3 \cdot 2MeOH$ were grown by slow diffusion of diethyl ether into a saturated solution of the complex in methanol. Slow evaporation of a solution of **3**$(CF_3SO_3)_4$ in methanol gave crystals of the monohydrate of this compound. Single crystals of **2**(CF_3SO_3) were selected from the recrystallized bulk product. Crystal data and details of the data collection and refinement for each compound

(17) Anderson, S. N.; Basolo, F. In *Inorganic Syntheses*; Kleinberg, J., Ed.; McGraw-Hill: New York, 1963; p 216.
(18) Dixon, N. E.; Lawrence, G. A.; Lay, P. A.; Sargeson, A. M. *Inorg. Chem.* **1984**, *23*, 2940.
(19) Turner, P. C.; McLennan, A. G.; Bates, A. D.; White, M. R. H. *Instant Notes in Molecular Biology*; Bios Scientific Publishers: Oxford, 1997; p 40.
(20) Jenkins, T. C. In *Drug−DNA Interaction Protocols*; Fox, K. R., Ed.; Humana Press: Totowa, NJ, 1997; p 195.

Table 1. Crystallographic Data for **1**$(CF_3SO_3)_3$·2MeOH, **2**(CF_3SO_3), and **3**$(CF_3SO_3)_4$·H_2O

	1$(CF_3SO_3)_3$·2MeOH	**2**(CF_3SO_3)	**3**$(CF_3SO_3)4$·H_2O
empirical formula	$C_{10}H_{35}F_9N_7O_{11}RhS_4$	$C_{20}H_{23}F_3N_4O_3S_2$	$C_{23}H_{40}F_{12}N_9O_{13}RhS_5$
fw	831.60	488.54	1141.85
T, K	228(2)	223(2)	223(2)
λ, Å	0.71073	0.71073	0.71073
space group	*C*2/*c*	$P\bar{1}$	$P\bar{1}$
a, Å	29.230(6)	9.504(2)	12.088(1)
b, Å	9.832(3)	11.4557(9)	12.314(1)
c, Å	22.802(8)	11.550(3)	15.675(1)
α, deg	90.00	64.23(1)	108.658(7)
β, deg	100.02(2)	80.82(2)	97.767(7)
γ, deg	90.00	75.12(1)	97.660(7)
V, Å^3	6453(3)	1092.8(3)	2151.1(3)
Z	8	2	2
ρ(calcd), g cm^{-3}	1.712	1.485	1.763
abs coeff, mm^{-1}	0.894	0.300	0.758
abs correction	empirical	none	integration
$2\theta_{max}$, deg	50.70	50.68	55.00
final *R* indices [$I > 2\sigma(I)$]	R1[a] = 0.0564	R1 = 0.0565	R1 = 0.0431
	wR2[b] = 0.1334	wR2 = 0.1144	wR2 = 0.0884
no. of data/restraints/params	5883/18/449	3702/23/346	9321/-/638
R indices (all data)	R1 = 0.0898	R1 = 0.1008	R1 = 0.0673
	wR2 = 0.1521	wR2 = 0.1328	wR2 = 0.0979

[a] $R1 = \sum||F_o| - |F_c||/\sum|F_o|$. [b] $wR2 = [\sum[w(F_o^2 - F_c^2)^2]/\sum w(F_o^2)^2]^{1/2}$.

are summarized in Table 1. Data were collected on a computer-controlled Bruker AXS P4 autodiffractometer using ω scans and graphite-monochromated Mo Kα radiation. The structures were solved with the Bruker AXS SHELXTL-PC (version 5.10) software package using direct methods techniques. The resulting structural parameters have been refined to convergence using counterweighted full-matrix least-squares techniques. The structural models incorporated anisotropic thermal parameters for all non-hydrogen atoms and isotropic thermal parameters for all included hydrogen atoms. The ammine hydrogen atoms in **1**$(CF_3SO_3)_3$·2MeOH and **3**$(CF_3SO_3)_4$·H_2O were located from a difference Fourier map and included in the structural model as rigid rotors (using idealized sp^3-hybridized geometry and N−H bond lengths of 0.90 Å). Hydrogen atoms H1N and H2N in **2**(CF_3SO_3) were located from a difference Fourier map and refined as independent isotropic atoms. Additional information on refinement procedures and treatment of positional disorders has been deposited as Supporting Information in CIF file format. All calculations were performed using the SHELXTL-PC (version 5.10) interactive software package (G. Sheldrick, Bruker AXS, Madison, WI).

Photolyses. Potentiometric measurements were performed using an Accumet AR 25 pH/ion meter equipped with an Accumet ammonia ion selective electrode (ISE no. 69494). A 1.0 mM solution of **1**(CF_3SO_3) in 50 mM phosphate buffer (pH 7.6) was continuously irradiated with UVA−vis light (150 W Xe arc lamp, 360−600 nm short-pass filter, Oriel). Samples of 1000 μL were taken at selected time points, and concentrations of free ammonia were determined following the instructions provided by the electrode manufacturer. ^{1}H and ^{15}N{^{1}H} NMR measurements were performed on solutions of **1**(CF_3SO_3) and **1***(CF_3SO_3) (25 mM rhodium, 0.1 M phosphate buffer, pH* 7.9) in D_2O or 5% D_2O/95% H_2O, respectively, after suitable time periods of irradiation (0−24 h) in 5 mm NMR tubes. Reported data are averages of three measurements.

DNA Binding Assays. Calf thymus DNA [10^{-4} M (bp)] was incubated with **1**(CF_3SO_3) and **3**$(CF_3SO_3)_4$ in TE buffer (10 mM Tris base, 1.0 mM EDTA, pH 7.4) at varying concentrations of rhodium complex (10−200 μM). The concentration range was limited by precipitation of the DNA at [Rh] > 200 μM. The mixtures were irradiated for 24 h at room temperature using a 450 W Hg medium-pressure light source (ACE). Dark controls were incubated for 24 h at room temperature. Unbound rhodium was removed by exhaustive dialysis against a minimum of 5 L of TE buffer in a 28-well microdialysis system (Gibco BRL) at 4 °C in the dark. The DNA samples were digested in 4 M HCl at 55 °C for 24 h and analyzed for rhodium content using ICP-AES. Experiments were performed in duplicate.

DNA Photocleavage Assays. Samples were prepared in 10 mM Tris buffer (pH 7.8) and contained 10^{-4} M (bp) pUC19 plasmid DNA and 50 μM rhodium complexes or free acridine. Photolyses were carried out in quartz fluorescence cells using a 200 W Hg-(Xe) light source (Oriel) equipped with a 360−600 nm short-pass filter. Samples (100 μL) of the continuously irradiated solutions were removed at each time point and stored at −20 °C. DNA single- and double-strand breaks were detected by gel electrophoresis assays through 5 mm, 1% agarose gels using 10 mM TAE (Tris−acetate−EDTA) running buffer (pH 8.0). Gels were run at 4 °C in the dark for 7 h at 46−50 V, stained with aqueous ethidium bromide (0.5 μg/mL), and photographed on Polaroid 667 film. Bands in scanned photographs of the gels were quantified using the Gel-Pro Analyzer software (version 3.1, Media Cybernetics, Des Moines, IA). The reduced ability of ethidium bromide to intercalate into supercoiled plasmid (form I) was accounted for by dividing the corresponding band intensities by 0.77.[21]

Cytotoxicity Assays. HL-60 leukemia cells were maintained in RPMI-1640 growth medium containing 10% heat-inactivated fetal bovine serum. Stock solutions (1.0 mM) of all compounds were made in saline. The photocytotoxicity of **1**$(CF_3SO_3)_3$, **2**(CF_3SO_3), and **3**$(CF_3SO_3)_4$ was assessed using a soft agar clonogenicity assay. Cells growing in log phase were treated with drug at varying concentrations, exposed to light (250 W Xe arc, λ > 360 nm) for 0.5 h, and incubated for another 3.5 h at 37 °C in a CO_2 incubator. Controls were included both of cells incubated for 4 h in the dark and of cells exposed to light for 0.5 h in the absence of drugs. Cells from each treatment were washed drug-free, resuspended in growth medium containing 0.3% Bacto Agar, and incubated in quadruplicate in humidified air at 37 °C for 7 days. Colonies (>15 cells/colony) were scored using an inverted light microscope. IC_{50}

(21) Herzberg, R. P.; Dervan, P. B. *J. Am. Chem. Soc.* **1982**, *104*, 313.

Scheme 1[a]

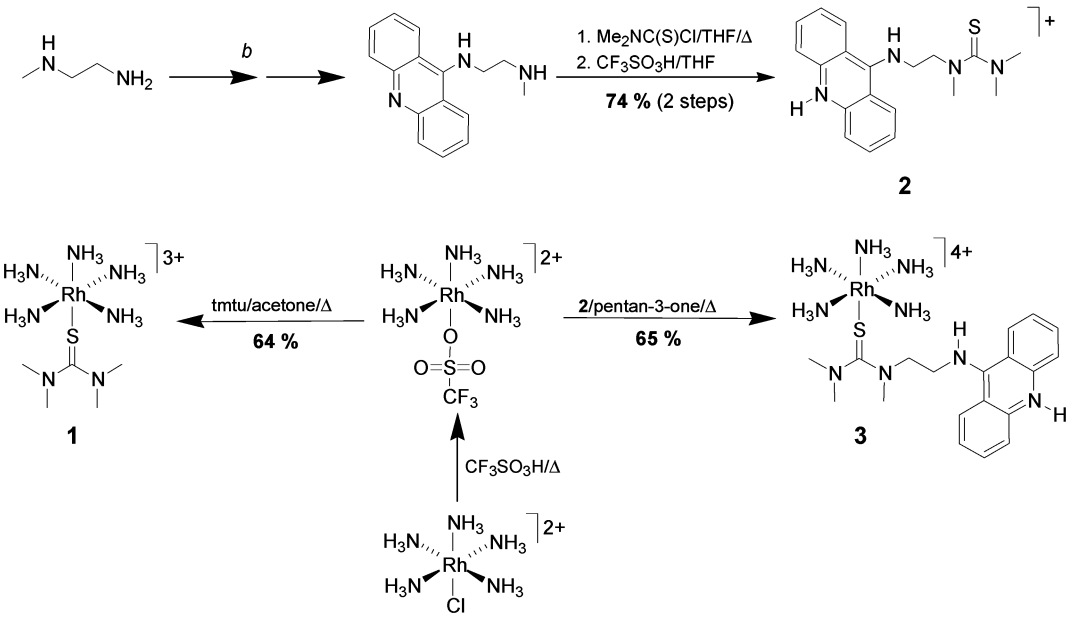

[a] Counterions and crystal solvents not shown. [b]Reagents and conditions: (1) CF_3COOEt/THF/0 °C; (2) $(Boc)_2O$/THF/<10 °C; (3) NaOH/MeOH/rt; (4) 9-PhOAcr/PhOH/Δ; HCl, AcOH/rt; (6) 2 M NH_3.

data (drug concentration at which colony growth was inhibited by 50%) were calculated as a percentage of control cells from logarithmic plots of drug concentration vs the average of four colony counts.

Results and Discussion

Design Rationale. In a suitably modified rhodium(III) pentaammine, $[Rh(NH_3)_5L]^{3+}$ (L = DNA-affinic carrier system), ligand-field photolysis would result predominantly in the dissociation of ammine ligands, while the intercalator-based carrier system would remain attached to the metal during the activation of the compound on target DNA. The rationale behind this approach is that intercalative preassociation in addition to electrostatic binding would prevent the formation of, likewise inert, photohydrolysis products and instead favor direct binding of the rhodium center to nucleophilic donor groups of the biomolecule. In rhodium complexes of the type $[Rh(NH_3)_5X]^{n+}$, where X is a donor that is considerably lower in the spectrochemical series than ammine, e.g., Br^- or I^-, photolabilization of NH_3 trans to X on the tetragonal (weak) axis is observed.[22] We therefore decided to use sulfur in acridinylthiourea (sulfur is a weak-field donor[23]) to produce the "light-resistant" linkage between metal and intercalator.

Synthesis and Characterization. The synthetic pathways for the rhodium complexes and the acridine-based carrier system are summarized in Scheme 1. The sulfur-modified rhodium pentaammine $[Rh(NH_3)_5(tmtu)]^{3+}$ (**1**) was synthesized by substitution of the "labile" triflato ligand[24] in $[Rh(NH_3)_5(OSO_2CF_3)](CF_3SO_3)_2$ with sulfur ligand.[25] The acridinylthiourea 1-[2-(acridin-9-ylamino)ethyl]-1,3,3-trimethylthiourea was synthesized from the 9-aminoacridine precursor *N*-acridin-9-yl-*N*′-methylethane-1,2-diamine and isolated as the hydrotriflate salt **2**(CF_3SO_3). **2** contains a tetraalkylated thiourea moiety that is thermally more robust than partially alkylated thioureas (e.g., in ACRAMTU; see Chart 1), which tend to undergo metal-mediated desulfurization.[26] The synthesis involved selective protection/deprotection of the primary and secondary amino groups in *N*-methylethylenediamine, attachment of the primary amino group to the 9-position of acridine via nucleophilic aromatic substitution, and transformation of the dangling secondary amine into thiourea. Finally, linkage of carrier ligand **2** to rhodium pentaammine was achieved by a procedure similar to that described for **1**$(CF_3SO_3)_3$. However, substitution of triflate in $[Rh(NH_3)_5(OSO_2CF_3)](CF_3SO_3)_2$ by **2** required extended reaction times and the use of a high-boiling-point solvent. The reduced rate of substitution in this system compared to the analogous reaction with tmtu is most likely the result of unfavorable electrostatic interactions between the cationic reactants. All target compounds were fully characterized by ^1H NMR and UV−vis spectroscopy, combustion analyses (see the Experimental Section), and single-crystal X-ray crystallography.

Views of the cations $[\mathbf{1}]^{3+}$, $[\mathbf{2}]^{+}$, and $[\mathbf{3}]^{4+}$ in the solid state are shown in Figures 1−3. Selected bond lengths and angles are given in Table 2. Trivalent rhodium in **1** and **3** is coordinated by five ammine ligands and the sulfur atom of the respective thiourea derivative. In both cases, the steric bulk of peralkylated thiourea causes deviations from ideal

(22) Skibsted, L. H. *Coord. Chem. Rev.* **1989**, *94*, 151.
(23) Huheey, J. E.; Keiter, E. A.; Keiter, R. L. *Inorganic Chemistry*; Harper Collins: New York, 1993; pp 405−408.
(24) Dixon, N. E.; Lawrence, G. A.; Lay, P. A.; Sargeson, A. M. *Inorg. Chem.* **1983**, *22*, 846.
(25) The choice of the noncoordinating solvent acetone proved to be critical. From analogous reactions in DMF/methanol only the solvent adduct $[Rh(NH_3)_5(OHCNMe_2)](CF_3SO_3)_3 \cdot MeOH$ was isolated (Turney, E. C.; Day, C. S.; Bierbach, U. Unpublished crystal structure).
(26) Brader, M. L.; Ainscough, E. W.; Baker, E. N.; Brodie, A. M. *Polyhedron* **1989**, *8*, 2219.

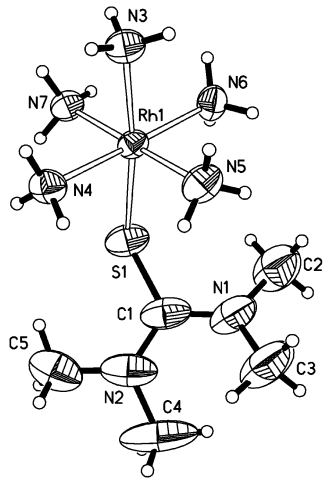

Figure 1. ORTEP presentation of the cation of **1**$(CF_3SO_3)_3$·2MeOH in the solid state giving atom numbering. Ellipsoids are drawn at the 50% probability level.

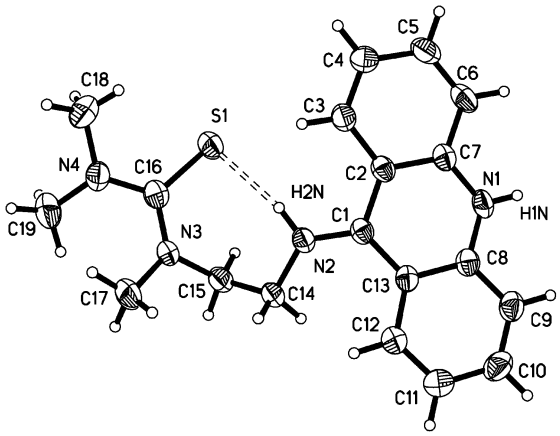

Figure 2. ORTEP presentation of the cation of **2**(CF_3SO_3) in the solid state giving atom numbering. Ellipsoids are drawn at the 50% probability level. The dashed bond indicates an intramolecular hydrogen bond contact.

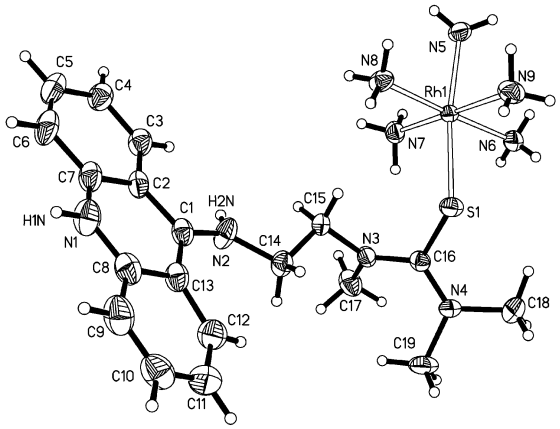

Figure 3. ORTEP presentation of the cation of **3**$(CF_3SO_3)_4$·H_2O in the solid state giving atom numbering. Ellipsoids are drawn at the 50% probability level.

octahedral geometry around the metal center. In **1** and **3**, the Rh−N bonds trans to thiourea show a slight, but significant, lengthening due to the static trans effect of sulfur [**1**, Rh−N_{trans} 2.100(5) Å vs Rh−N_{cis} 2.078(5) Å (mean); **3**, Rh−N_{trans} 2.094(3) Å vs Rh−N_{cis} 2.072(3) Å (mean)]. This perturbation of the electronic ground state, which is reflected in ^{15}N NMR chemical shifts observed for the isotopically labeled analogue **1***, does not result in increased thermal hydrolysis of the trans Rh−N bond (vide infra). This is in contrast to the situation in structurally related tmtu-substituted Pt(IV) complexes, which undergo rapid hydrolysis in the dark.[27] A comparison of the structures of unmodified and rhodium-modified acridinylthiourea provides insight into the conformational flexibility of the carrier ligand. In **2**, the ethylene bridge connecting the bulky thiourea and acridine residues is in a gauche conformation that is stabilized by a weak hydrogen bond involving thiourea sulfur and the exocyclic 9-amino group (see Figure 2; N2−H2N---S1 3.210(4) Å). Metalation of the sulfur atom results in the disruption of this intramolecular contact and an elongated structure of the conjugate (Figure 3). The advantages of a flexible polymethylene linker chain in acridinylthioureas with respect to DNA binding and biological activity have been demonstrated recently for analogous bifunctional platinum−acridines.[15]

The UV−vis spectrum of **1**$(CF_3SO_3)_3$ exhibits a strong absorbance at 250 nm, assigned to the $\pi \rightarrow \pi^*$ transition within tmtu,[28] and a low-intensity band at 378 nm (Figure 4). The latter feature is assigned to the lowest-energy LF transition, $\pi(d_{xz},d_{yz}) \rightarrow \sigma^*(d_{z^2})$, under C_{4v} symmetry of the

Table 2. Selected Bond Lengths (Å) and Angles (deg) for Cations **1**−**3**

		1	
Rh1−N3	2.100(5)	Rh1−N6	2.077(5)
Rh1−N4	2.077(5)	Rh1−N7	2.079(5)
Rh1−N5	2.082(5)	Rh1−S1	2.378(2)
S1−C1	1.735(8)	N1−C1	1.360(11)
N2−C1	1.342(10)		
N6−Rh1−N4	178.7(2)	N7−Rh1−N3	88.8(2)
N6−Rh1−N7	89.3(2)	N5−Rh1−N3	88.9(2)
N4−Rh1−N7	90.6(2)	N6−Rh1−S1	93.73(17)
N6−Rh1−N5	92.1(2)	N4−Rh1−S1	87.56(16)
N4−Rh1−N5	87.9(2)	N7−Rh1−S1	82.99(16)
N7−Rh1−N5	177.2(2)	N5−Rh1−S1	99.28(18)
N6−Rh1−N3	88.3(2)	N3−Rh1−S1	171.48(17)
N4−Rh1−N3	90.3(2)	C1−S1−Rh1	115.1(3)
		2	
N3−C16	1.353(5)	N4−C16	1.352(4)
S1−C16	1.688(4)		
N4−C16−N3	17.7(3)	N4−C16−S1	120.7(3)
N3−C16−S1	121.6(3)		
		3	
Rh1−N5	2.094(3)	Rh1−N8	2.081(3)
Rh1−N6	2.064(3)	Rh1−N9	2.073(3)
Rh1−N7	2.070(3)	Rh1−S1	2.354(1)
S1−C16	1.730(3)	N3−C16	1.349(4)
N4−C16	1.325(4)		
N6−Rh1−N7	87.65(15)	N6−Rh1−S1	88.34(11)
N6−Rh1−N9	91.01(16)	N7−Rh1−S1	98.75(10)
N7−Rh1−N8	92.24(15)	N9−Rh1−S1	82.36(11)
N9−Rh1−N8	89.05(16)	N8−Rh1−S1	94.05(10)
N6−Rh1−N5	88.76(15)	N7−Rh1−N9	178.23(16)
N7−Rh1−N5	89.51(15)	N6−Rh1−N8	177.60(16)
N9−Rh1−N5	89.31(16)	N5−Rh1−S1	171.13(12)
N8−Rh1−N5	88.84(14)	C16−S1−Rh1	116.29(12)
N4−C16−N3	119.4(3)	N4−C16−S1	118.3(3)
N3−C16−S1	122.2(3)		

(27) Bierbach, U.; Hambley, T. W.; Roberts, J. D.; Farrell, N. *Inorg. Chem.* **1996**, *35*, 4865.
(28) Gosavi, R. K.; Rao, C. N. R. *Can. J. Chem.* **1967**, *45*, 1897.

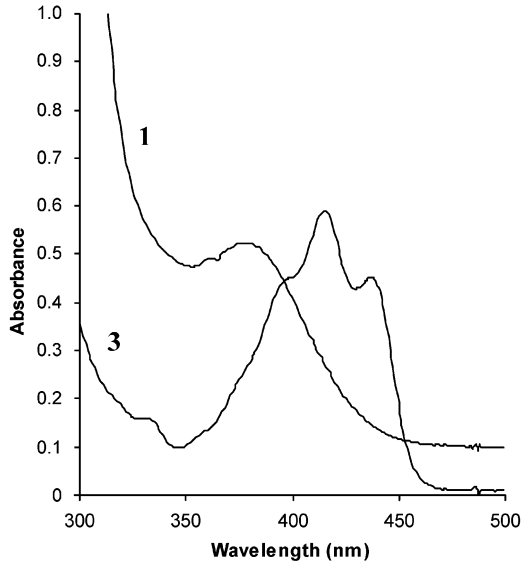

Figure 4. Electronic absorption spectra of aqueous solutions of **1**$(CF_3SO_3)_3$ (10^{-3} M) and **3**$(CF_3SO_3)_4$ (6×10^{-5} M).

complex ion.[29] In conjugate **3**, this LF transition is obscured by strong absorption maxima in the 350−450 nm range resulting from $\pi \rightarrow \pi^*$ transitions within the acridine chromophore (Figure 4). The consequences of this spectral overlap for the DNA interactions and photobiology of **3** will be addressed in the following sections.

Photochemistry of the [RhN$_5$S] Moiety. The ligand-field photolysis of **1** was monitored by electroanalytical measurements and ^{1}H NMR spectroscopy. In addition, photosubstitution and photoisomerization reactions of the rhodium pentaammine were studied by ^{15}N{^{1}H} NMR spectroscopy using the analogous ^{15}N-labeled complex [Rh($^{15}NH_3$)$_5$(tmtu)]$^{3+}$ (**1***). Light with $\lambda > 360$ nm was used to avoid Rh(III)/Rh(II) redox chemistry originating from ligand-to-metal charge-transfer (LMCT) excited states.[30] In the presence of light, rhodium releases 2 equiv of ammine ligand during the first 12 h of continuous irradiation at room temperature and neutral pH. While the first equivalent of ammine ligand was released in less than 1 h, the second hydrolysis step appeared to be considerably slower (Figure 5). ^{1}H NMR spectra (not shown) taken of photolyzed reaction mixtures during this time period showed no indication of release of tmtu, on the basis of the absence of the signal for the methyl protons in free tmtu (δ 3.06). A decrease of the singlet peak at δ 3.22 (tmtu CH_3 in **1**) and the appearance of two major peaks at δ 3.21 and 3.19 was observed, suggesting the formation of new rhodium species containing coordinated tmtu. ^{15}N{^{1}H} NMR spectroscopy confirmed the release of ammine ligands during the photolysis of **1*** and gave additional information on the nature of the photohydrolysis products. Measurements were taken at various time points during the first 24 h of irradiation (selected spectra are shown in Figure 6). The decrease of the signals of the

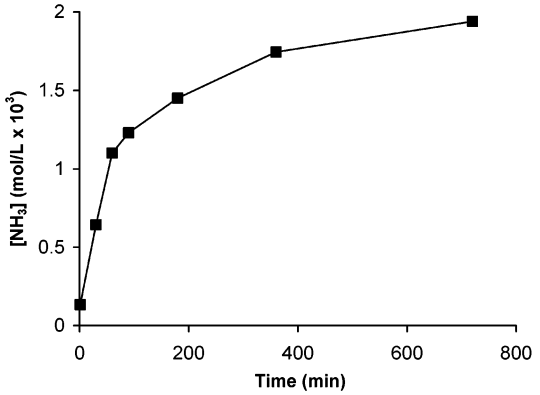

Figure 5. Photolysis of **1**$(CF_3SO_3)_3$ (10^{-3} M complex, 0.05 M phosphate buffer, pH 7.6) with 360−600 nm light monitored by ion selective electrode measurements.

starting material at δ −53.54 and −61.96 (the splitting into doublets results from ^{15}N−^{103}Rh coupling) was accompanied by the appearance of a singlet at δ −1.74, assigned to free $^{15}NH_3$. In addition, multiple doublets appeared in the −50 to −80 ppm region (Table 3), indicating formation of a complex product mixture. A distinct difference in ^{15}N chemical shifts and heteronuclear coupling constants is seen for axial $^{15}NH_3$ trans to thiourea sulfur, which is high in the trans influence series, and mutually trans-oriented (equatorial) $^{15}NH_3$ in **1***. In a series of complexes of the type [Rh($^{15}NH_3$)$_5$Z]$^{n+}$,^{15}N chemical shifts and the magnitude of one-bond coupling constants, ^1J(^{15}N−^{103}Rh), have been shown to correlate with the trans influence of the ligand Z.[31] In general, a downfield shift of the ^{15}N resonance and a decrease in heteronuclear coupling ^1J are observed with increasing labilization of the Rh−N$_{trans}$ bond.[31] Thus, the relative order of trans influences of the ligands involved, thiourea S > NH_3 > H_2O/OH^- (potentially phosphate O), was useful for the assignment of ^{15}N resonances in the photohydrolysis products (Table 3). On the basis of the various physical data, a mechanism of photohydrolysis is suggested (Scheme 2) that involves rapid dissociation of ammine trans to sulfur and isomerization of the primary hydrolysis product, which slowly undergoes secondary hydrolysis from a photostationary equilibrium.[32] The release of ammine ligand trans to sulfur rather than from an equatorial position would be expected on the basis of the relative order of ammine and thiourea in the spectrochemical series. Solutions of **1**/**1*** irradiated for >12 h showed formation of a yellow precipitate, indicating that further decomposition of the primary hydrolysis products occurs. The latter observation is supported by the ^{15}N{^{1}H} NMR data, on the basis of the multiplicity of signals assigned to metal-bound ammine. All of the above experiments were performed with "dark controls". None of the reactivity features described were observed in the absence of light.

Covalent DNA Interactions. To assess the overall DNA binding affinity of **1** and **3**, the rhodium complexes were incubated with native, random-sequence DNA for 24 h at

(29) Petersen, J. D.; Watts, R. J.; Ford, P. C. *J. Am. Chem. Soc.* **1976**, *98*, 3188.
(30) Horvath, O.; Stevenson, K. L. *Charge-Transfer Photochemistry of Coordination Compounds*; VCH Publishers: New York, 1993; p 296.
(31) Appleton, T. G.; Hall, J. R.; Ralph, S. F. *Inorg. Chem.* **1988**, *27*, 4435.
(32) Skibsted, L. H. *Coord. Chem. Rev.* **1989**, *94*, 151.

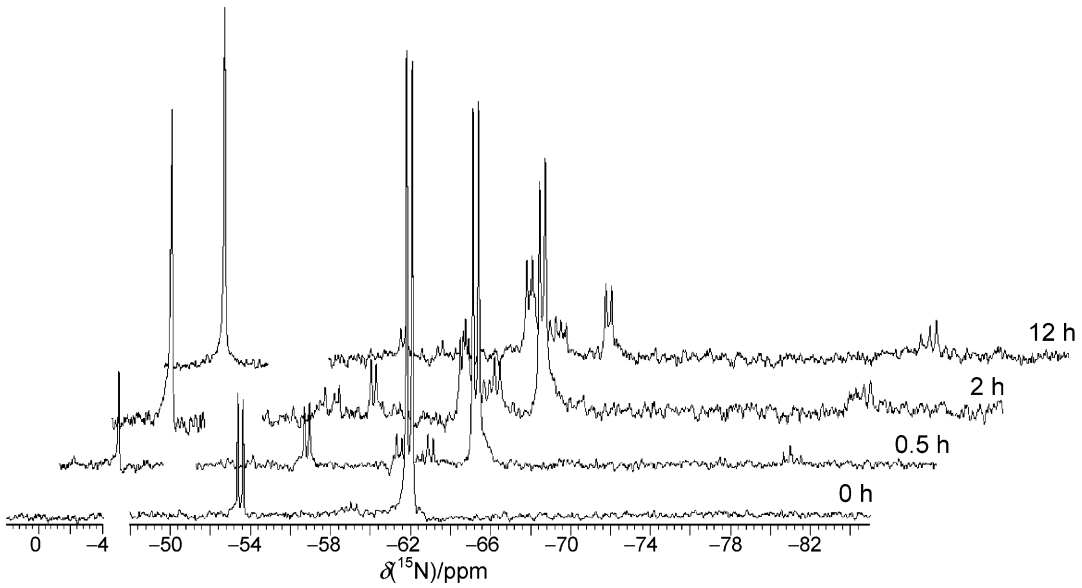

Figure 6. Photohydrolysis and photoisomerization reactions of **1***$(CF_3SO_3)_3$ monitored by proton-decoupled ^{15}N NMR spectroscopy (50.7 MHz, 95% H_2O/5% D_2O, [Rh] = 25 mM, 0.1 M phosphate, pH* 7.9).

Table 3. $^{15}N\{^1H\}$ NMR Data for Photolysis Products of **1***

$\delta_{^{15}N}$ (ppm) [$^1J(^{15}N-^{103}Rh)$ (Hz)]	assignment
−1.74	$^{15}NH_3/^{15}NH_4^+$
−50.98 [12.5], −51.72 [12.9]	$H_3{}^{15}N-Rh-S$
−53.54 [12.5][a]	
−58.00 [13.4], −58.14 [13.9],	$H_3{}^{15}N-Rh-N$
−59.17 [13.9], −59.70 [13.9]	
−61.96 [13.4][a]	
−77.44 [16.2], −77.56 [17.6],	$H_3{}^{15}N-Rh-O$
−77.68 [15.7], −78.17 [16.3]	

[a] Unreacted **1***.

Scheme 2. Proposed Mechanism of Photoaquation of **1**

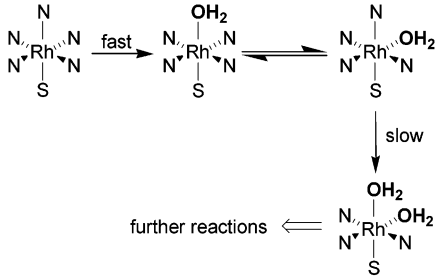

room temperature both with light and in the dark. Concentrations of rhodium ranged from 10 to 200 μM. The amount of metal covalently associated with DNA was determined by atomic emission spectrometry after exhaustive dialysis and acidic digestion of the samples and is reported as r_b values (metal-to-nucleotide ratios) in Figure 7. Under thermal conditions, the degree of DNA modification by **1** and **3** was, as expected, considerably lower than in the case of divalent

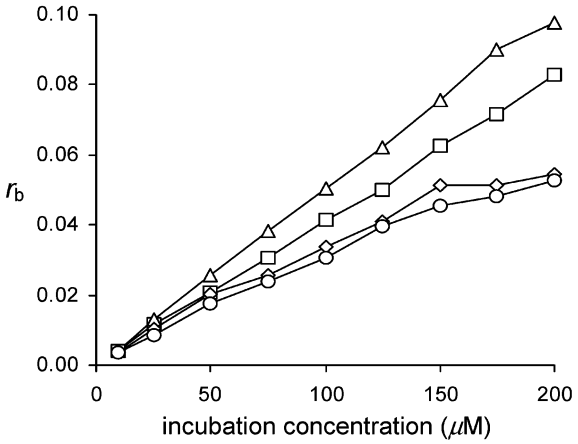

Figure 7. Degree of modification of calf thymus DNA as a function of rhodium concentration for **1**, dark (○), **1**, *hν* (◇), **3**, *hν* (□), and **3**, dark (△). Conditions: [DNA] = 10^{-4} M (base pairs), TE buffer (10 mM Tris/1 mM EDTA, pH 7.4), 24 h irradiation, 450 W Hg medium-pressure light source, $\lambda > 350$ nm. R_b = [Rh]/[DNA nucleotides].

platinum.[16] At a drug concentration of 100 μM, for instance, conjugate **3** metalated 1 in 20 nucleotides while structurally related PT−ACRAMTU (Chart 1) modified one-third of the DNA bases ($r_b \approx 0.3$) under the same conditions. In our experiments, the DNA-affinic acridine carrier resulted in slightly higher binding levels for rhodium in **3** relative to the nontargeted metal in **1**. Surprisingly, unlike BISPHEN,[11] none of the derivatives showed light-enhanced metalation, and binding levels were largely independent of irradiation times (data not shown). Binding levels for **3** were consistently lower in the light than in the dark (see the following section for a plausible explanation). While no DNA adducts were detected for BISPHEN in the dark at 37 °C,[11] a low degree of DNA modification is observed for **1** and **3**. Rhodium pentaammine appears to be more accessible to DNA binding sites than the bulky phenanthroline compound. The fact that **1** and **3** produce covalent adducts in the absence of light is somewhat surprising. One possible explanation would be that

the trans influence of sulfur, although not favoring thermal hydrolysis, may facilitate dissociation of ammine in reactions with strong DNA nucleophiles.

DNA Photocleavage. Contrary to our predictions, the degree of covalent modification of DNA by **1** and **3** did not indicate light-enhanced binding. Instead, DNA photocleavage was observed when rhodium was incubated with closed-circular supercoiled plasmid DNA. While oxidative DNA photocleavage by rhodium(III)- and ruthenium(II)-based metallointercalators via direct hydrogen abstraction from the deoxyribose residue or base oxidation is well-established, DNA strand breakage by simple nonintercalating rhodium ammines, such as **1**, is unprecedented. Agarose gel electrophoresis showed that **1** induced single-strand breaks (Figure 8a) while **3** produced almost complete degradation of plasmid after 24 h (Figure 8c). No cleavage activity was observed in the dark (gels not shown). DNA strand scission by **1** was not affected by excess dmso (a hydroxyl radical scavenger), sodium azide (a singlet oxygen quencher), and catalase, which suggests an oxygen-independent cleavage mechanism (Figure 8b).[33] Figure 8c provides important information on the DNA interactions of rhodium−acridine: the reduced electrophoretic mobility of the plasmid and the resolution of form I DNA into topoisomers in lane 2 are suggestive of a dual binding mode that involves a combination of irreversible covalent binding and intercalation.[16] Nicking of the relaxed topoisomers by **3** was observed after 30 min of irradiation, leading to the open-circular form of the plasmid. The increase in electrophoretic mobility of this band (lane 3) suggests that the rhodium−DNA linkage is slowly reversed, resulting in the dissociation of the 4+ cation from DNA. This effect and the loss of rhodium bound to low-molecular-weight DNA fragments during dialysis would explain the relatively low binding levels in irradiated samples compared to nonirradiated samples of **3** (Figure 7).

As discussed above, selective irradiation into the metal-based band was not feasible, due to the overlap of the UV−vis features of the acridine chromophore with the LF transition of rhodium. To assess whether the carrier ligand in **3** contributes to the DNA cleavage activity of the conjugate, acridine **2** alone was studied under the same conditions. Surprisingly, **2** was found to cause efficient nicking of plasmid and induced double-strand breaks as evidenced by the appearance of a band assigned to linearized plasmid (lanes 5−10 in Figure 8d). Figure 8e shows that linear DNA forms before all of the supercoiled form is converted to open-circular plasmid. The coexistence of all three forms of DNA in lanes 5 and 6 and the fact that a sharp band is observed for form III may indicate that the formation of the linear DNA is a nonrandom process initiated by a single molecule.[34] Further statistical tests,[35] however, have to be applied to substantiate this notion. The efficient degradation of plasmid by light-activated **3** is most likely due to the combined cleavage activity of rhodium and the acridine chromophore. The experiments also demonstrate the limited utility of acridine as a DNA-affinic carrier system in hybrid agents, if selective activation of the non-acridine moiety in the 350−450 nm range is desired. Various papers[36]

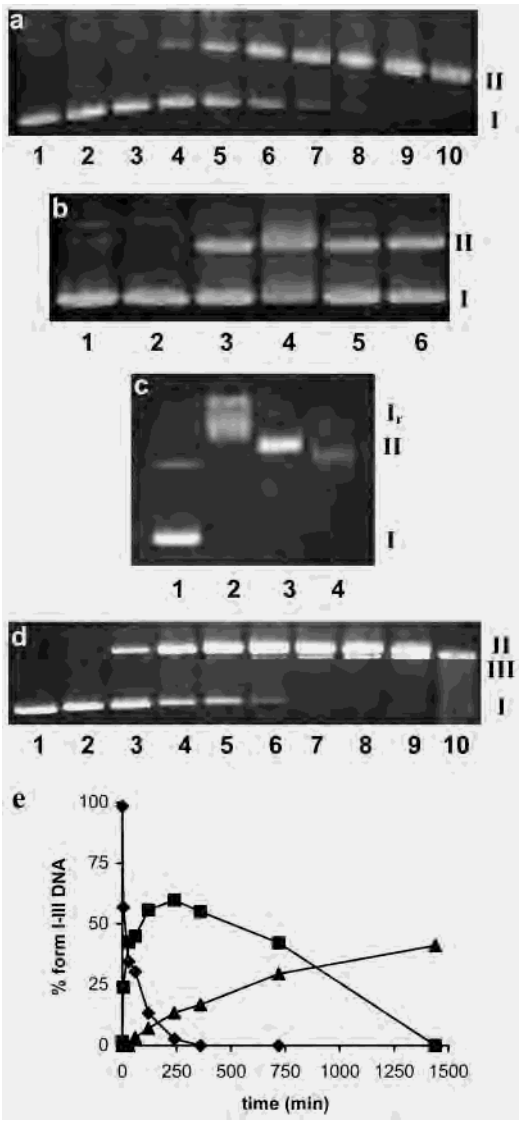

Figure 8. Light-induced DNA strand breaks in pUC19 plasmid caused by **1**$(CF_3SO_3)_3$, **2**(CF_3SO_3), and **3**$(CF_3SO_3)_4$ monitored by agarose gel electrophoresis. Incubation conditions: [Rh] = 50 μM, [DNA] = 10^{-4} M (bp), 10 mM Tris buffer (pH 7.8), 200 W Xe(Hg) arc lamp, $\lambda > 360$ nm, ambient temperature. Lanes: **(a)** (1) pUC19 irradiated for 24 h in the absence of **1**$(CF_3SO_3)_3$, (2) 0 min, (3) 5 min, (4) 30 min, (5) 1 h, (6) 2 h, (7) 4 h, (8) 6 h, (9) 12 h, (10) 24 h. **(b)** (1) pUC19 plasmid, (2) pUC19 treated with **1**$(CF_3SO_3)_3$ for 1 h, no *hν*, (3) pUC19 treated with **1**$(CF_3SO_3)_3$ for 1 h, *hν* (4) 1 h, *hν* + 1000 units mL^{-1} catalase, (5) 1 h, *hν* + 50 mM DMSO, (6) 1 h, *hν* + 50 mM NaN_3. **(c)** (1) pUC19 in the absence of **3**$(CF_3SO_3)_4$, (2) pUC19 incubated with **3**$(CF_3SO_3)_4$ for 15 min in the dark, (3) *hν*, 30 min, (4) *hν*, 24 h. No cleavage activity is observed in the dark (not shown). **(d)** (1) pUC19, (2) pUC19 + **2**(CF_3SO_3), 0 min, (3) 5 min, *hν*, (4) 30 min, *hν*, (5) 1 h, *hν*, (6) 2 h, *hν*, (7) 4 h, *hν*, (8) 6 h, *hν*, (9) 12 h, *hν*, (10) 24 h, *hν*. DNA forms: I, closed-circular plasmid, supercoiled; Ir, closed-circular plasmid, relaxed topoisomers; II, nicked open-circular plasmid; III, linearized plasmid. **(e)** Quantitation of the three forms of DNA in (d) at various irradiation times: ◆, closed-circular, supercoiled (form I); ■, nicked open-circular (form II); ▲, linear (form III).

(33) Armitage, B. *Chem. Rev.* **1998**, *98*, 1171.
(34) Melvin, M. S.; Tomlinson, J. T.; Saluta, G. R.; Kucera, G. L.; Lindquist, N.; Manderville, R. A. *J. Am. Chem. Soc.* **2000**, *122*, 6333.
(35) Freifelder, D.; Trumbo, B. *Biopolymers* **1969**, *7*, 681.
(36) (a) Theodorakis, E. A.; Xiang, X.; Blom, P. *Chem. Commun.* **1997**, 1463. (b) Nakatani, K.; Shirai, J.; Sando, S.; Saito, I. *Tetrahedron Lett.* **1997**, *38*, 6047.

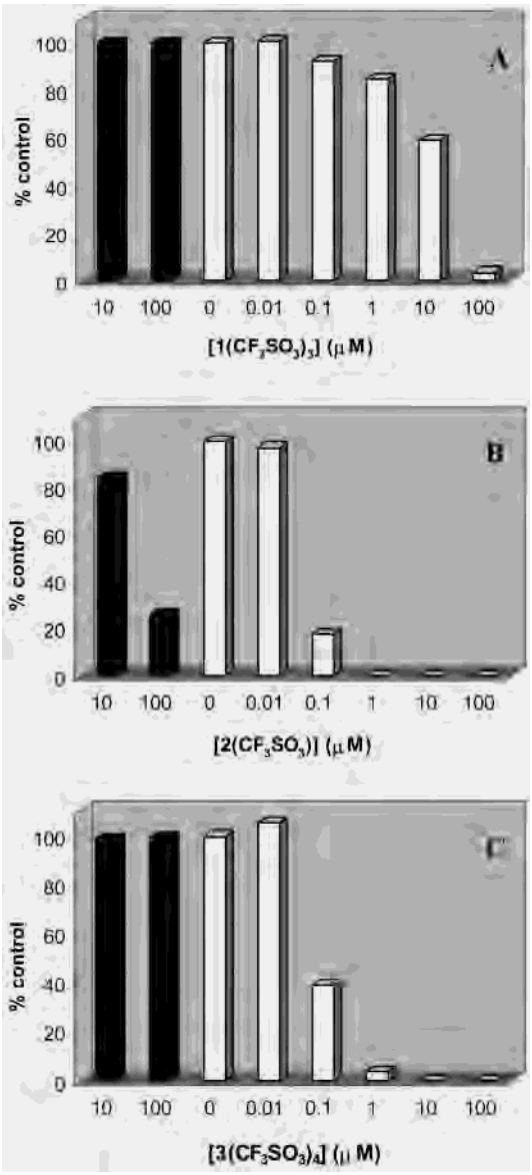

Figure 9. Cytotoxicity data for **1**$(CF_3SO_3)_3$ (A), **2**(CF_3SO_3) (B), and **3**$(CF_3SO_3)_4$ (C) in human leukemia HL-60. Black columns represent dark controls. White columns represent incubations of cells with rhodium at varying concentrations with 30 min light exposure (see the Experimental Section for details).

have appeared in the literature describing enhancement of DNA photocleavage by tethering cleaving agents to the intercalator 9-aminoacridine. Our data suggest that the acridine chromophore itself can give rise to photoinduced DNA strand scission, which may have been overlooked in previous studies.

Photocytotoxicity. To assess whether the photoreactivity and DNA-damaging properties of **1**−**3** produce an in vitro effect, preliminary cytotoxicity data were generated in HL-60 leukemia cells using a clonogenic survival assay. The data are summarized in bar charts A, B, and C in Figure 9. The rhodium compounds **1** and **3** were noncytotoxic in the dark. In both cases, no cell kill was observed at incubation concentrations as high as 100 μM. After exposure of the drug-treated cells to light for 30 min, nontargeted complex **1** inhibited cell growth by 50% at a concentration (IC_{50}) of 20 μM. Under the same conditions, complex **3** proved to be approximately 450 times more potent than **1** (the IC_{50} for **3** was 0.044 μM). Similar to **3**, unmodified acridine **2** resulted in light-induced cell kill at nanomolar concentrations (IC_{50} = 0.011 μM). **2** also produced moderate culture growth inhibition in the dark at drug levels similar to those observed for ACRAMTU (Chart 1).[15] Interestingly, attachment of rhodium to sulfur in **2** appears to mask the dark toxicity of the 9-aminoacridine derivative. This effect, which cannot be rationalized at this point, renders **3** a genuine "light-only" cytotoxic agent. Possible covalent DNA adducts formed by **1** and **3**, as suggested by the r_b levels established in calf thymus DNA, have to be considered noncytotoxic. Finally, the IC_{50} values established for **1**−**3** appear to correlate with the extent of DNA damage observed in photocleavage assays. Complex **1**, which produces single-strand breaks, was only moderately active in vitro. In contrast, **2** and **3**, which are more efficient at producing DNA cleavage—possibly involving DNA double-strand breaks—were highly cytotoxic. DNA double-strand breaks are known to be more cytotoxic due to the fact that they are repaired less efficiently by the cell than single-strand breaks.[37] More work, however, has to be done to prove the causal relationship between in vitro DNA damage and the extent of cell kill. Additional experiments have to be carried out to demonstrate that the agents are actually delivered to the nucleus and cell death is caused by damage of chromosomal DNA.

Conclusions and Perspectives

We have proposed a new strategy for activating inert metal ammines in biological matrixes. UVA radiation can be used to "switch on" the DNA cleavage chemistry and cytotoxicity of the rhodium−acridine complex **3**. Such compounds have potential applications as biochemical tools (e.g., as photofootprinting agents) or in the photodynamic therapy (PDT) of cancer. The latter treatment modality, however, would be limited to topical cancers, due to the inability of UVA radiation to deeply penetrate tissue.[38] Overlap of the electronic spectra of the individual components of this hybrid agent did not allow selective activation of the metal without "turning on" the photochemistry of the intercalator, which complicates mechanistic studies of the metal−DNA interactions. Thus, future work will be concerned with extending the metal−acridine concept to kinetically inert longer-wavelength metals, such as cobalt(III), chromium(III), osmium(III), and related ions. Analogous sulfur-modified pentaammines of these metals are expected to undergo ligand-field hydrolysis in the 500−600 nm range,[18] which would allow selective activation of the metal moiety. The DNA photocleavage data for **1** suggest that strand scission by rhodium(III) is not mediated by singlet oxygen or diffusible hydroxyl radicals. Future mechanistic work will explore the possibility of a Lewis acid-catalyzed hydrolytic

(37) Weaver, D. T. *Trends Genet.* **1995**, *11*, 388.
(38) Henderson, B. W.; Dougherty, T. J. *Photochem. Photobiol.* **1992**, *55*, 145.

cleavage mechanism[39] that is promoted by the electrophilic attack of light-activated rhodium on the phosphodiester DNA backbone.

Acknowledgment. This work was supported by the Academic Research Initiation Grants Program (Grant 2001-ARG-0010) of the North Carolina Biotechnology Center (NCBC) and the Science Research Fund of Wake Forest University. We thank Dr. Marcus W. Wright for his assistance with the $^{15}N\{^{1}H\}$ NMR experimental setup. A generous loan of rhodium(III) chloride from Johnson Matthey PLC (Reading, U.K.) is also gratefully acknowledged.

Supporting Information Available: X-ray crystallographic data for the structure determinations of **1**$(CF_3SO_3)_3 \cdot 2MeOH$, **2**(CF_3SO_3), and **3**$(CF_3SO_3)_4 \cdot H_2O$ in CIF format. This material is available free of charge via the Internet at http://pubs.acs.org.

IC025744N

(39) Sreedhara, A.; Cowan, J. A. *J. Biol. Inorg. Chem.* **2001**, *6*, 337.